Highly Flexible Crash Barriers

Dr. Paul Heyliger
John Kienholz
Charlie McLean
Fernando Ramirez

Department of Civil Engineering
Colorado State University
Fort Collins CO 80523

May 2004

Acknowledgements

Disclaimer

Abstract

A preliminary study modeling the nonlinear behavior of long, slender wooden members was conducted at Colorado State University to evaluate their use in inexpensive, destroyable crash barriers. This preliminary study compared the results of physical test data, published exact solutions, and the solutions of a numerical model all with respect to simple, two-dimensional elastica frames.

The results have varying levels of agreement that nonetheless give credibility to the performance of the numerical method. The research shows that the numerical model is ready to be expanded to model three-dimensional elastica frames.

TABLE OF CONTENTS

Executive Summary

Wood is a desirable building material because it is relatively inexpensive and widely available. Though it is widely used in stiff structures with tight serviceability requirements, it is generally unused in cases where the structure is desired to have a relatively low stiffness and have large deformations or even break altogether. Inexpensive wooden crash barriers could be designed to absorb the energy from an impact and protect the more expensive object or vehicle hitting it. The crash barrier could then be cheaply replaced or left to biodegrade if need be.

The goal of this project was to learn to model two-dimensional frames of long, slender wooden members and compare them to published results and data gathered from physical experiments. This study was done using three different frames – a rigid-node square loaded at opposite midspans in tension, a diamond frame with two rigid nodes and loaded at opposite pin connections in tension, and a slightly more complicated three-bay by three-bay frame.

The results of the physical experiments and the numerical model have satisfactory levels of agreement with published data while the results of the three-bayed frame and the model have good qualitative agreement. Though the results are not perfect, there is significant evidence validating the numerical model. The next step in this project would be to expand the numerical model to three dimensions and to compare the results to more physical experiments.

1. Introduction

In nearly all applications of wood for use as structural components, deflections of wood trusses, beams, or frames are limited to infinitesimal amounts. This is usually because serviceability of wood structures demands high stiffness and low displacement load-deformation characteristics so that bridges do not sag under load and residential houses do not sway in the wind. Yet there are other applications of wood structural members, which as a class have seen very little exploration and study, that could benefit from having a relatively low stiffness, thereby yielding a "soft" structure that has a load-deformation properties that exploit the ability of the structure to store strain energy as it goes through large deformations. Highly flexible wood networks have a limited but unexplored range of applications given the huge prevalence of wood structural members in the United States. For many of these applications, they are extremely well suited, and it is possible that even more structural systems could be envisioned with similar characteristics. In this research, the fundamental mechanics of these structural wood systems are studied using computational techniques and static measurements. (Dynamic testing was not done, contrary to what was stated in the proposal)

Before describing the key elements of the research, it is first useful to describe what is meant by a large deformation in a wood element. When structural elements are loaded, they deform. This deformation within the solid leads to strains, usually qualified as small or infinitesimal. Small strains combined with small displacements usually result in a deformed structure that looks, to the naked eye, exactly the same as the undeformed structure. The strains are then linked with internal stresses via the wood constitutive behavior, and when these stresses are integrated over an interior region of the wood structural element, their resultants sum to resist the applied load. This basic mechanism is what happens in a large percentage of wood structural elements when loaded under given design specifications. However, significant changes in analysis are required when considering similar systems under large deformations.

This report outlines the accomplishments that took place during the summer of 2003. The following describes tasks completed as part of a study that will be continued by others. The purpose of this summer's activities was to test the Fortran code created by Fernando Ramirez and determine how well it predicted the behavior of multi-member frames by comparing its results to those of experiments and published solutions when applicable.

2. Literature Review

Although the majority of wood structures and systems are designed and analyzed by small deformation, small strain linear analysis, there is significant literature on the nonlinear analysis of wood and wood structures. The vast majority of these studies focus on some of the dominant sources for nonlinear response within a structure, including but not limited to material nonlinearity in the constitutive law, stick-slip behavior during contact between two wood elements, P-Delta effects from second-order analysis, and inclusion of von Karman nonlinearity for moderately large deformations in beams. Kingston and Budgen [1] presented one of the first nonlinear analyses of the rheological behavior of wood under high stresses in bending and compression. Maghsood *et al* [2] constructed early nonlinear finite element models of structural wood members for use in many different applications. Sheathed wood diaphragms also possess strongly nonlinear behavior, and were studied by Itani and Cheung [3]. Polensek and Kazic [4] studied the reliability of wood composites in the nonlinear range of behavior.

Several studies have been devoted to the load-slip behavior of connections in wood-metal joints. Gebremedhin *et al* [5] examined metal plate connected wood joints loaded in-plane, and Groom and Polensek [6] studied the nonlinear behavior of truss-plate joints. Another area of study with strong nonlinear components are light-fame stud walls, which have been studied by Kasal and Leichti [7] Kasal, Leichti, and Itani, [8] Groom and Leighti, [9] Tarabia and Itani, [10] and Waltz *et al* [11]. The nonlinear behavior of layered wood systems and wood composites have been studied by Wheat and Calixto [12] and Davids [13]. Examples of the influence of nonlinear material behavior in wood include studies by Lang and Wolcott [14] for viscoelastic consolidation, Holmberg *et al* [15] has studied general nonlinear mechanical behavior, and a nonlinear orthotropic finite element model was developed by Tabiei and Wu [16].

Slender wood elements can exhibit nonlinear response characteristics, especially when loaded dynamically. Tesar [17] has examined the vibration of slender bridges using nonlinear elements, and Filiatrault and Folz [18] examined seismic design under such conditions. Other dynamic loadings include guardrail systems (an example suggested by this proposed study), which has seen initial tests by Plaxico, Ray, and Hiranmayee [19]. Shear walls can also undergo nonlinear response under what would be called usual operating conditions, and have been recently studied by Ceccotti and Karacabeyli [20] and Andreasson *et al* [21]. There are a number of other studies of this subject, and this review has been representative but not exhaustive. Other works of a similar nature are also mention in Pellicane [22]. There have also been several exact closed-form solutions to general elastica problems by Jenkins [23] and Kerr [24], both of which we make use of during our evaluation of our computational algorithm.

3.   Theory

3.1   The Elastica Wood Element

The vast majority of structural wood studies completed to date that have modeled wood components as one-dimensional fibers have used the assumptions associated with small displacement Euler-Bernoulli beam theory combined with linear structural analysis. This implies a number of assumptions regarding the behavior of the line element. Most notably, 1) the kinematic hypothesis of classical beam theory requires that plane sections of the beam cross section remain plane and perpendicular to the centroidal axis of the beam, 2) the stress-strain law is one-dimensional and is caused by deformation of the line element center combined with either stretch or compression of either side of the element, and 3) the displacements and strains are infinitesimal. This allows the equations of equilibrium to be reduced to a single, fourth-order ordinary differential equation relating the transverse load q to the transverse displacement w

$$\frac{d^2}{dx^2}\left(EI\frac{d^2w}{dx^2}\right) = q$$

(Equation 1)

Here E is the Young's modulus of the fiber along its long axis and I is the bending moment of inertia. Hence all material properties and geometric parameters are condensed into two scalar quantities.

For the usual deformation of wood elements, the restriction that the beam displacements are small is accurate for most phenomena, such as small amplitude vibrations or normal building analysis. However, in these applications, it is very likely that the wood element will be deformed into a position for which this equation is invalid. This is because the mathematical relationship between the bending moment M in the cross-section of the fiber and the curvature k of the deformed element can be expressed for linear analysis as

$$\kappa = \frac{1}{\rho} = \frac{M}{EI}$$

(Equation 2)

The exact mathematical link between the curvature and the transverse displacement of the line element w is given by

$$\kappa = \frac{\frac{d^2w}{dx^2}}{\left[1 + \left(\frac{dw}{dx}\right)^2\right]^{\frac{3}{2}}}$$

(Equation 3)

When the displacements and displacement gradients are infinitesimal, the slope of the deformed wood element is very small compared to unity, and hence the denominator above is nearly one. In this case, the curvature reduces to the linear differential equation

$$\frac{M}{EI} = \frac{d^2w}{dx^2}$$

(Equation 4)

However, for an arbitrary loading of a wood element (or a collection of such elements) under large deformations, this relationship is not valid under the most general loading conditions. In the present application of narrow wood elements as structural members, the elements undergo very large deformations where the slope of the line element is not small, but the strain is still infinitesimal. The reason for this is that in beam bending, the axial strain along the element, given by the ratio of the distance from the centroid and the radius of curvature, varies linearly with distance y from the tube center. If the wood element radius is small, the radius of curvature must also be extremely small before the stresses in the wood reach or exceed the elastic limit. Because of the mechanics of deformation, then, the nonlinear term in the equation of curvature must be included in the analysis, thereby complicating the formulation.

It is proposed to model the wood elements or assembly of elements as a network of elastica, each with the capability to withstand large deformations but only small strains for the reasons outlined above. This basic problem was first proposed and studied by Euler, who in fact coined the name "elastica" and provided the first solutions. Even the simplest elastica geometry admits analytic solution only using elliptic integrals, which must generally be evaluated numerically. In this proposal, each wood element is formulated as an elastica, with possible junctions where two or more elements cross, forming an elastica wood frame.

3.2   Variational Formulation and Finite Element Model

The variational formulation and corresponding finite element model of the frame as represented by the elastica is based on treating wood elements as a one-dimensional continuum, with the vast bulk of the energy stored by extension/contraction and flexure of the element. Because of the inherently nonlinear behavior of the response of the elastica to external load, the nonlinear curvature term in the expression for the strain energy must be considered. This requires minimization of the strain energy of the element represented by the elastica, given as

$$\pi = \int_L \frac{EIw''}{[1 + w'^2 R]^{\frac{5}{2}}} dx$$

(Equation 5)

where L is the length of the beam, w is the transverse beam displacement, R the radius of curvature, EI the beam stiffness, and x the beam axial coordinate. There have been several studies that have constructed the finite element model of individual elastica, but usually only for very special two-dimensional loading conditions of individual elastica. The method used in this work is aimed at determining the nonlinear curvature by a sequence of incremental changes to the beam geometry through inclusion of the axial force term in the potential energy statement. This approach has been used by Yang [25] for two-dimensional geometries. The strain energy due to small bending and using Green's strain tensor is given by

$$U = \frac{1}{2} \int_0^L EA \left(\frac{\partial u}{\partial x} \right)^2 dx + \frac{1}{2} \int_0^L EI \left(\frac{\partial^2 w}{\partial x^2} \right)^2 dx + \frac{S}{2} \int_0^L \left[\left(\frac{\partial w}{\partial x} \right)^2 + \left(\frac{\partial u}{\partial x} \right)^2 \right] dx$$

(Equation 6)

where u is now the beam axial displacement and S the axial force along the beam centroidal axis. The curvature expression in the second integral is not exact, but is an excellent approximation to the curvature if w is much smaller than the beam length.

6

Using the finite element approach where x is always in a local coordinate system of the one-dimensional elements, the partial derivatives become complete and the variation of the strain energy becomes

$$\delta U = \int_0^L \frac{du}{dx} EA \frac{d\delta u}{dx} dx + \int_0^L \frac{d^2w}{dx^2} EI_z \frac{d^2\delta w}{dx^2} dx + S \int_0^L \left(\frac{du}{dx} \frac{d\delta u}{dx} + \frac{dw}{dx} \frac{d\delta w}{dx} \right) dx$$

(Equation 7)

The shape functions, as well as the development of the elastic stiffness matrix, K_e, can be seen in Yang. Using these shape functions in each term of Equation 7, we can get the stiffness matrix and the geometric stiffness matrix. See Appendix A for the development of the geometric stiffness matrix, K_G. Under initial loading, the second integral is non-zero under bending, and the first and third integrals are exactly zero since the transverse and axial components of displacement uncouple. As the geometry changes, all terms become non-zero, and the axial stiffening and updated geometry couple to provide an excellent approximation to the exact deformation. This is accomplished through a linearized incremental formulation by which the standard stiffness matrix is modified by changes in the geometry. The code used in this project is based on one such method as outlined in the text by Yang and Kuo [26].

4. Physical Models

4.1 Nodes

Our two-dimensional physical models are the diamond, the square, and the 3x3 bay frame. In all models, the members are made of 1/8th-inch diameter wooden dowels. In all the models, a rigid connection between members is needed to transfer forces and movents. A few different methods of achieving these rigid nodal connections were attempted. A successful connection would be one where failure of the member occurs before yielding or failure at the node. The node is considered to have yielded or failed if the angle between the members changes or if one of the members slips relative to the other.

The first attempts were using different adhesives, wood glue and an epoxy called Hardman Adhesives made by Elements Performance Polymers. The wood glue proved to yield before the members did. The main difficulty with the Hardman Adhesives is the fact that the glue is too viscous and will flow away from its desired location, not enough stays near the node to help transfer the forces.

The node connection that was finally decided upon performed very well, but will have some drawbacks in the long run. These nodes are comprised of small cubes of wood that are approximately 5/8 inches to a side. Small holes slightly larger than the members were drilled through each face slightly off the cube's center. This connection does introduce some eccentricities to the structure, but not much more than those using an epoxy for the connection, see Figure 1. The eccentricity also allows the members to be continuous through the node, even when expanding the concept to three dimensions. A small amount of tape was then used to secure the nodes in place and prevent them from sliding along the member, allowing for transfer of shear and axial forces between the members.

This connection has a few advantages over a connection where glue is involved. When assembling a three-dimensional structure, one can visualize the difficultly in keeping all the members in their proper place while applying the adhesives and while they dry. With the wooden node, the frame can be moved around and adjusted throughout the assembly process. Once the assembly is complete, there is no period of down time while the connections set.

However, the current node has some disadvantages. The connections are limited to orthogonal directions. Future applications may require members joining at different angles. This may be addressed by using a spherical node, or a node with more sides. These types of nodes will require more time to produce and will be more difficult to manufacture quickly and easily without some creativity.

4.2 Diamond

A simple two-dimensional diamond frame was tested to explore how the code predicted behavior of multi-member frames. The diamond had two fixed connections and two pinned connections, each across from the other. The frame was loaded by pulling (tension) on the two pin connections. The diamond frame's exact solution was found using elliptical integrals as shown in the paper by Yang.

9

The pinned connections were made by lining up two nodes and sliding a short dowel through the third dimension hole. Tape was used to secure the member dowels to the node. This was done at both ends of each member to prevent them from being pulled out of the node. However, at the pin connections, no tape was used on the short dowel that connects the two halves of the diamond. This allowed them to rotate freely.

4.3   Square

The square frame was much simpler. It had four rigid connections and was loaded in tension at the mid-span of two opposing members. The square was made using four dowels of equal length and four of the same wooden nodes, creating a square where all connections are rigid. The exact solution for this test was also found in Yang's Paper.

4.4   Three-Bay Frame

The three-bay frame was assembled using eight 30-inch dowels and 16 nodes. The four vertical and four horizontal dowels are then evenly spaced and tape was used to keep the dowels fixed to the nodes. Then, small cones were affixed along the top and bottom nodes. This helped the square nodes act more like pins as the load is applied and the nodes rotated.

5.   Testing the Physical Models

5.1   Modulus of Elasticity

Before we could compare our numerical results to those of experiments, we had to have a value for the Young's Modulus of the wooden dowels. This value was not taken from design books because of the high factor of safety imbedded into wood design codes and there are many unknowns surrounding the purchased dowels – species, grade, age, moisture content, etc. – that made choosing a published value difficult. The modulus of elasticity was found using the average of five samples. Each sample was created by gluing six short dowels around each end of a longer dowel and allowing them to dry for a several days. The purpose of this is to try to prevent the main dowel from being damaged by the grips. The Instron machine was then used to acquire data relating load and displacement.

5.2   Diamond

The top pin connection was held in place at the top of the Instron machine. A small, light container was affixed to the bottom pin connection so ball bearings could be added individually to load the frame. The movable base of the Instron was used to measure the deflection after each ball bearing was added. After each weight was added, the base was moved by hand until the marker lined up again with the center of the node. See Figure 2. The deflection could then be read and recorded from the Instron's control panel.

5.3   Square

The mid-span of the top member was held at the top of the Instron machine. A small, light container was affixed to the bottom member at mid-span so ball bearings could be added individually to load the frame. Again, the movable base of the Instron was used to measure the deflection after each ball bearing was added. After each weight was added, the base was moved by hand until the marker lined up again with the midspan of the lower member. See Figure 3. The deflection could then be read and recorded from the Instron's control panel.

5.4   Three-Bay Frame

The testing apparatus is more than three feet long and four feet high. The apparatus has plexiglass on both sides so that the frame could be seen during the loading. The Instron machine was used in conjunction with a 1,000-pound load cell to test the three-bay frame. The device used to keep the frame two-dimensional was too big to fit inside testing machine. To circumvent this problem, a lever system, as seen in Figure 4, was rigged so the contraption could be set up in front of the machine and the load applied via the lever.

This setup allowed the loading rate to be controlled much more effectively and made it possible to record much of the non-linear portion of the frame's load vs. deflection curve. The lever system required that the raw data retrieved from the Instron machine be adjusted to give accurate results. The load was halved and the displacement was doubled since the location of applied load was at mid-span of the lever. Elastic deformation of the lever was assumed to be negligible.

6. Results

6.1   Modulus of Elasticity

Load-Deflection curves were found for each specimen using the Instron machine and, from this data, stress-strain curves were created knowing, each specimen's length and cross-sectional area. Wood does not have a distinct linear region and yielding point like steel does. Hence, only the initial portion of the curves which is nearly linear was used to find the slope and, hence, the modulus of elasticity. See Figure 5 for an example and Table 1 for the results.

As one can see, the data is variable but stays close to an average near 1500 ksi. Hence, this value was used in the code.

6.2   Diamond

The results from the diamond frame are shown in Figure 6. The exact solution was taken from the paper by Jenkins. The code was run using double symmetry and 10 elements for the member that was modeled.

6.3   Square

The results from the testing of the square frame are shown in Figure 7. In the code, the double symmetry was not used and all four members were modeled using 10 elements per side.

6.4   Three-Bay Frame

Using the method of testing discussed above, reasonable, but not perfect, data has been found for frame strength. The testing results give a P-Delta curve that match expected characteristics. These results can be seen in Figure 8. However, the predicted P-Delta curve from the code does not match the experimental results. It can be seen that the experimental data is slightly stiffer than the code predicts it should be.

7.   Discussion and Conclusions

7.1   Code

The code used for this project, originally written by co-author Fernando Ramirez, needed some improvement to work for all materials and member sizes. It was found that the code worked fine for materials with very high strength and large size, but would not work for wooden dowels (low strength) and small sizes (thin dowels), which was needed for this project.

It was first thought that the strength and material size had a large influence on the condition number of matrices in the code. If the condition number is too large the computer is not able to accurately solve the large matrices involved in a finite element analysis. After looking deep into this problem it was found that the condition number of the matrices in the code was not what was causing the problem. However it was still evident that larger numbers for strength would make the code work. To tackle this problem, all the units of force and length were changed at the beginning of the code effectively, turning small numbers for strength into large numbers so that the code would work. The code only sees numbers, not what units they are in. After the code was done with all of its analysis the results were converted back to the correct units to give accurate results. This method of solving the problem worked for all frames within extremely large and extremely small frame properties.

7.2   Diamond

Looking at Figure 6, one can see that the code and the exact solution as presented by Yang have excellent agreement. The experimental results, however, do not match well. It is found that they differ by a factor of nearly two. This discrepancy is believed to be the result of a difference in the definition of the length L or in the load P. However, after diligent searching, the discrepancy has not yet been resolved. It is known that the definition of L as published in the paper by Yang differs from the definition of L as published in the paper by Jenkins, which Yang references. Yet their solutions are in agreement. Hence, Jenkins' definition of L was used in this project and it was determined that Yang was in error. This discovery still does not resolve the issue.

7.3   Square

The results from the square model also have a few unresolved issues. The exact solution as published by Kerr [24] has good agreement with the experimental results, especially for the smaller displacements and loads. However, the exact solution and experimental results differ from the results of the code by a factor of the square root of 2. Again, the differences are believed to be in the definition of the length and load parameters. Yang defines L as the length of one side. However, Kerr defines L as half the length of a side because he uses the double symmetry in his solution to the elliptical integral and models only a quadrant of the square. Using this definition of L in the numerical analysis yields results that differ by roughly the square root of 2.

7.4 Three-Bay Frame

The experimental results and the output from the code tend to be in the same ballpark, but they are not perfect. There are two possible reasons for the discrepancy of results between the code and physical model: either the code is wrong or the there is something going wrong in the testing data. Something that could be wrong with the testing data is that there seems to be a substantial amount of friction in the testing device.

The friction between the glass and the nodes causes the data to be skewed in the stronger direction. It also causes some jumping in the data from the static friction being exceeded. It would seem that this friction would be negligible seeing as the friction between wood and plexiglass is not very large, but for a frame that can only hold a handful of pounds this friction significant. As for eliminating this friction, several methods have been tried and some are still being considered. One method is to constantly tap the glass with some sort of hammer as the frame is being loaded, this introduces a small vibration in the plexiglass and causes the nodes to slide more easily. Another method is to place a small dowel, sharpened on each side and slightly longer than a node is wide, through the hole in the third dimension of the node so that the when the frame is tested only these little points sticking out of the node slide against the plexiglass. These points did a wonderful job of smoothing out the data, however they failed to change the strength of the frame by a significant amount.

Other sources of friction could be between the loading block and the plexiglass, between the loading cell and the lever, between the lever and the loading block, and in the hinge at the end of the lever. Modifying each of these sources to make them frictionless would be a daunting task at best, especially since the exact amount of friction each source adds is unknown. Quantifying the amount of load that is added because of friction from these sources can be done by placing a scale on each end of the frame testing device and running a stiff rod between them and between the plexiglass for the frame to rest on. As the frame is loaded, the difference between half the value read from the Instron machine plus the loading block and the total value read from the two scales will be the amount of friction loss during the testing. Now the only friction unaccounted for will be that between the plexiglass and the stiff rod running between the scales.

This test was performed with a frame that had the sharpened dowels in the nodes and the plexiglass was tapped throughout the procedure. The test revealed that there was negligible friction from the entire testing device, the values from the load cell and the values from the scales were off by an average of less than two percent. This test showed that friction is not the problem in our testing device.

Many modifications to the code have been made from its original form to make it work for any reasonable frame size and material property. At this point, it is not believed that the discrepancies discussed above are due to an inherent flaw in the program itself. The high variability of the wooden dowels in strength and homogeneity make it almost impossible to line up physical data to exact solution. This could be a cause for some of the discrepancies, but this does not explain systematic differences, such as why the experimental results of the diamond frame differ from the code and exact solution roughly by a factor of two. These issues need to be resolved before continuing with the project.

The next step of this project will be expanding the code to three dimensions and testing a physical model in order to verify its results.

References

1. Kingston, R. S., and Budgen, B., "Some Aspects of Rheological Behavior of Wood 4. Nonlinear Behavior of High Stresses in Bending and Compression," *Wood Sci. Technol.* 6 (3), pp. 230 (1972).

2. Maghsood, J., Scott, N. R., Furry, R. B., "Linear and Nonlinear Finite-Element Analysis of Wood Structural members," *T. ASAE* 16 (3), pp.490-496 (1973).

3. Itani, R. Y., and Cheung, C. K., "Nonlinear-Analysis of Sheathed Wood Diaphragms," *J. Struct. Eng.-ASCE* 110 (9), pp. 2137-2147 (1984).

4. Polensek, A., and Kazic, M., "Reliability of Nonlinear Wood Composites in Bending," *J. Struct. Eng.-ASCE* 117 (6), pp. 1695-1702 (1991).

5. Gebremedhin, K. G., Jorgensen, M. C., and Woelfel, C. B., "Load-Slip Characteristics of Metal Plate Connected Wood Joints Tested in Tension and Shear," *Wood Fiber Sci.* 24 (2), pp. 118-132 (1992).

6. Groom, L., and Polensek, A., "Nonlinear Modeling of Truss-Plate Joints," *J. Struct. Eng.-ASCE* 118 (9), pp. 2514-2531 (1992)

7. Kasal, B., and Leichti, R. J., "Nonlinear Finite Element Model for Light-Frame Stud Walls," *J. Struct. Eng.-ASCE* 118 (11), pp. 3122-3135 (1992).

8. Kasal, B., Leichti, R. J., and Itani, R. Y., "Nonlinear Finite-element Model of Complete Light Frame Wood Structures," *J. Struct. Eng.-ASCE* 120 (1), pp. 100-119 (1994).

9. Groom, K., M., and Leichti, R. J., "Transforming a Corner of Light-Frame Wood Structure to a Set of Nonlinear Springs," *Wood Fiber Sci.* 26 (1), pp. 28-35 (1994).

10. Tarabia, A. M. and Itani, R. Y., "Static and Dynamic Modeling of Light-Frame Wood Buildings," *Comput. Struct.* 63 (2), pp. 319-334 (1997).

11. Waltz, M. E., McLain, T. E. and Miller, T. H., "Discrete Bracing Analysis for Light-Frame Wood-Truss compression in Webs," *J. Struct. Eng.-ASCE* 126 (9), pp. 1086-1093 (2000).

12. Wheat, D. L. and Calixto, J. M., "Nonlinear-Analysis of 2-Layered Wood Members with Interlayer Slip," *J. Struct. Eng.-ASCE* 120 (6), pp. 1909-1929 (1994).

13. Davids, W. G., "Nonlinear Analysis of FRP-Glulam-Concrete Beams with Partial Composite Action," *J. Struct. Eng.-ASCE* 127 (8), pp. 967-971 (2001).

14. Lang, E. M. and Wolcott, M. P., "A Model for Viscoelastic Consolidation of Wood-Strand Mats 2. Static Stress-Strain Behavior of the Mat," *Wood Fiber Sci.* 28a (3), pp. 369-379 (1996).

15. Holmberg, S., Persson, K., and Petersson, H., "Nonlinear Mechanical Behavior and Analysis of Wood and Fiber Materials," *Comput. Struct.* 72 (4-5), pp. 459-480 (1999).

16. Tabiei, A. and Wu, J., "Three-Dimensional Nonlinear Orthotropic Finite Element Material Model for Wood," *Comps. Struct.* 50 (2), pp. 143-149 (2000).

17. Tesar, A., "Vibration of New Types of Slender Wood Bridges," *Drev. Vysk.* 44 (3-4), pp. 1-19 (1999)

18. Filiatrault, A. and Folz, B., "Performance-Based Seismic Design of Wood-Framed Buildings," *J. Struct. Eng.-ASCE* 128 (1), pp. 39-47 (2002).

19. Plaxico, C. A., Ray, M. H. and Hiranmayee, K., "Impact Performance of the G4(1W) and G4(2W) Guardrail Systems - Comparison under NCHRP Report 350 Test 3-11 Conditions," *Transport. Res. Rec.* 1720 pp. 7-18 (2000).

20. Ceccotti, A. and Karacabeyli, E., "Validation of Seismic Design Parameters for Wood-Frame Shearwall Systems," *Can. J. Civil Eng.* 29 (3), pp. 484-498 (2002).

21. Andreasson S., Yasumura, M., and Daudeville, L., "Sensitivity Study of the Finite Element Model for Wood-Framed Shear Walls," *J. Wood Sci.* 48 (3), pp. 171-178 (2002).

22. Pellicane, P. J., "Modeling Considerations in Wood-Related Research," *J. Test. Eval.* 27 (1), pp. 69-68 (1999).

23. Jenkins, J. A., Seitz, T. B., and Przemieniecki, J. S., "Large Deflection of Diamond Shaped frames," *Int. J. Solids Struct.* 2, p. 591 (1966)

24. Kerr, C. N., "Large Deflections of a Square Frame," *J. Mech. and Applied Math* 17, p. 23-38 (1962)

25. Yang, T. Y., "Matrix Displacement Solution to Elastica Problems of Beams and Frames," *Int. J. Solids Structures* 9, p. 829-841 {1973}

26. Yang, Y. B., Kuo, S. R., <u>Theory and Analysis of Nonlinear Framed Structures</u>, Prentice Hall, New York, (1994)

Appendix A

Development of the Geometric Stiffness Matrix

The third term in Equation (7) can be split into two parts.

$$S \int_0^L \delta \left(\frac{du}{dx} \right)^2 dx = S \int_0^L \begin{bmatrix} -\frac{1}{L} \\ \frac{1}{L} \end{bmatrix} \begin{bmatrix} -\frac{1}{L} & \frac{1}{L} \end{bmatrix} dx = S \begin{bmatrix} \frac{1}{L} & -\frac{1}{L} \\ -\frac{1}{L} & \frac{1}{L} \end{bmatrix} \tag{8}$$

These terms become the entries, $K_{G,11}$, $K_{G,14}$, $K_{G,41}$, and $K_{G,44}$. These terms are zero if inextensibility is assumed, but this is not the case in this study. The second part fills in the rest of the geometric stiffness matrix.

$$S \int_0^L \delta \left(\frac{dv}{dx} \right)^2 dx = S \int_0^L \begin{bmatrix} -\frac{6x}{L^2} + \frac{6x^2}{L^3} \\ 1 - \frac{4x}{L} + \frac{3x^2}{L^2} \\ \frac{6x}{L^2} - \frac{6x^2}{L^3} \\ \frac{3x^2}{L^2} - \frac{2x}{L} \end{bmatrix} \begin{bmatrix} -\frac{6x}{L^2} + \frac{6x^2}{L^3} \\ 1 - \frac{4x}{L} + \frac{3x^2}{L^2} \\ \frac{6x}{L^2} - \frac{6x^2}{L^3} \\ \frac{3x^2}{L^2} - \frac{2x}{L} \end{bmatrix}^T dx \tag{9}$$

$$K_{G,22} = S \int_0^L \left(-\frac{6x}{L^2} + \frac{6x^2}{L^3} \right)^2 dx = \frac{1.2S}{L}$$

$$K_{G,23} = S \int_0^L \left(-\frac{6x}{L^2} + \frac{6x^2}{L^3} \right) \left(1 - \frac{4x}{L} + \frac{3x^2}{L^2} \right) dx = \frac{S}{10}$$

$$K_{G,25} = S \int_0^L \left(-\frac{6x}{L^2} + \frac{6x^2}{L^3} \right) \left(\frac{6x}{L^2} - \frac{6x^2}{L^3} \right) dx = -\frac{1.2S}{L}$$

$$K_{G,26} = S \int_0^L \left(-\frac{6x}{L^2} + \frac{6x^2}{L^3} \right) \left(\frac{3x^2}{L^2} - \frac{2x}{L} \right) dx = \frac{S}{10}$$

$$K_{G,33} = S \int_0^L \left(1 - \frac{4x}{L} + \frac{3x^2}{L^2} \right)^2 dx = \frac{2SL}{15}$$

$$K_{G,35} = S \int_0^L \left(1 - \frac{4x}{L} + \frac{3x^2}{L^2} \right) \left(\frac{6x}{L^2} - \frac{6x^2}{L^3} \right) dx = -\frac{S}{10}$$

$$K_{G,36} = S \int_0^L \left(1 - \frac{4x}{L} + \frac{3x^2}{L^2} \right) \left(\frac{3x^2}{L^2} - \frac{2x}{L} \right) dx = -\frac{SL}{30}$$

$$K_{G,55} = S \int_0^L \left(\frac{6x}{L^2} - \frac{6x^2}{L^3} \right)^2 dx = \frac{1.2S}{L}$$

$$K_{G,56} = S \int_0^L \left(\frac{6x}{L^2} - \frac{6x^2}{L^3} \right) \left(\frac{3x^2}{L^2} - \frac{2x}{L} \right) dx = -\frac{S}{10}$$

$$K_{G,66} = S \int_0^L \left(\frac{3x^2}{L^2} - \frac{2x}{L} \right)^2 dx = \frac{2SL}{15}$$

Again, the geometric stiffness matrix is symmetric and all other $K_{G,ij}$ entries are zero. The geometric stiffness matrix, K_G, becomes:

$$[K_G] = \begin{bmatrix} \frac{S}{L} & 0 & 0 & -\frac{S}{L} & 0 & 0 \\ 0 & \frac{1.2S}{L} & \frac{S}{10} & 0 & -\frac{1.2S}{L} & \frac{S}{10} \\ 0 & \frac{S}{10} & \frac{2SL}{15} & 0 & -\frac{S}{10} & -\frac{SL}{30} \\ -\frac{S}{L} & 0 & 0 & \frac{S}{L} & 0 & 0 \\ 0 & -\frac{1.2S}{L} & -\frac{S}{10} & 0 & \frac{1.2S}{L} & -\frac{S}{10} \\ 0 & \frac{S}{10} & -\frac{SL}{30} & 0 & -\frac{S}{10} & \frac{2SL}{15} \end{bmatrix}$$

(10)

The final stiffness matrix, K, is the sum of the elastic stiffness, K_e, and the geometric stiffness, K_G.

$$[K] = [K_e] + [K_G]$$

(11)

Appendix B

Tables and Figures

Modulus of Elasticity	
Sample	E (ksi)
1	1417
2	1532
3	1505
4	1576
5	1510
Average	1508

Table 1. Modulus of Elasticity Results
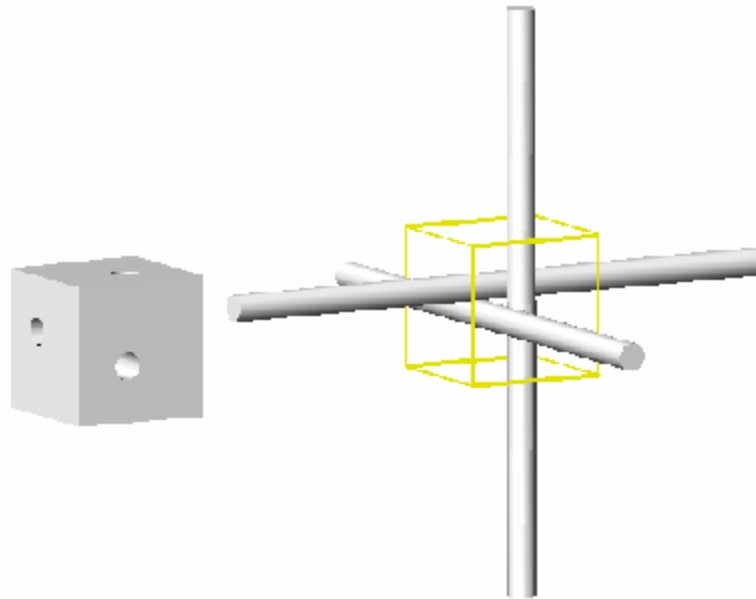
Figure 1. Nodal Connection
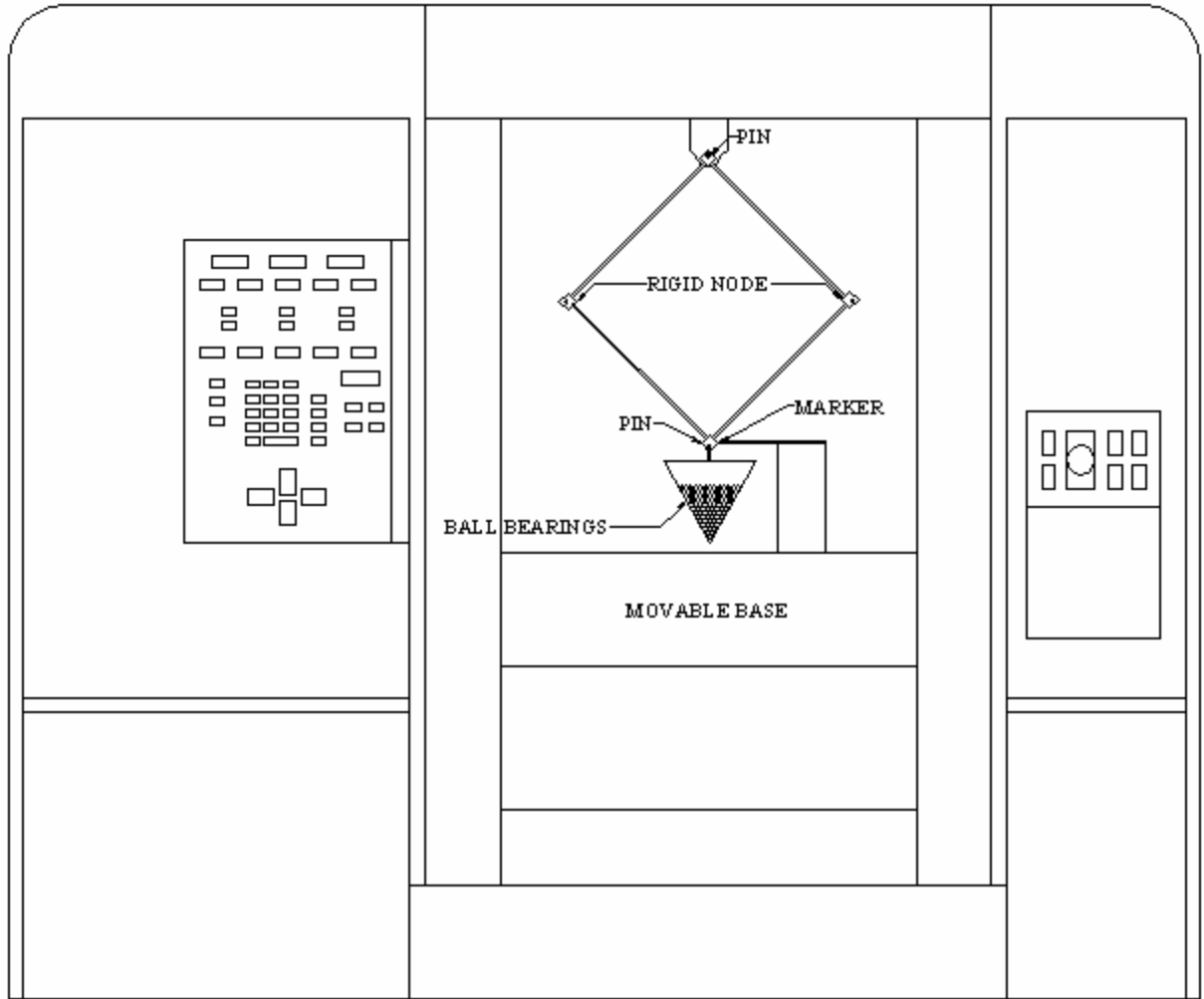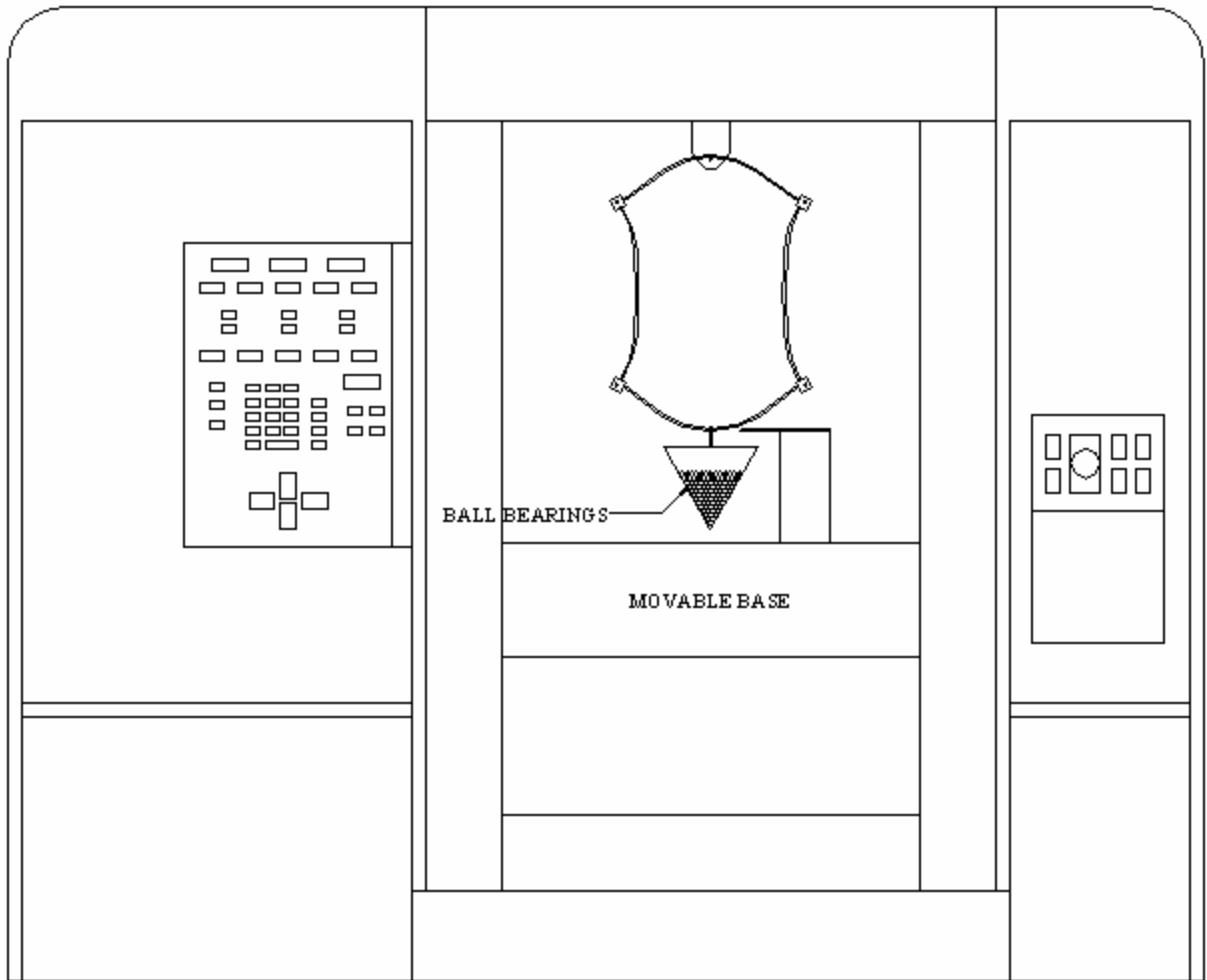
Figure 2. Experimental setup for the diamond frame

BALL BEARINGS

MOVABLE BASE

Figure 3. Experimental setup for the square frame
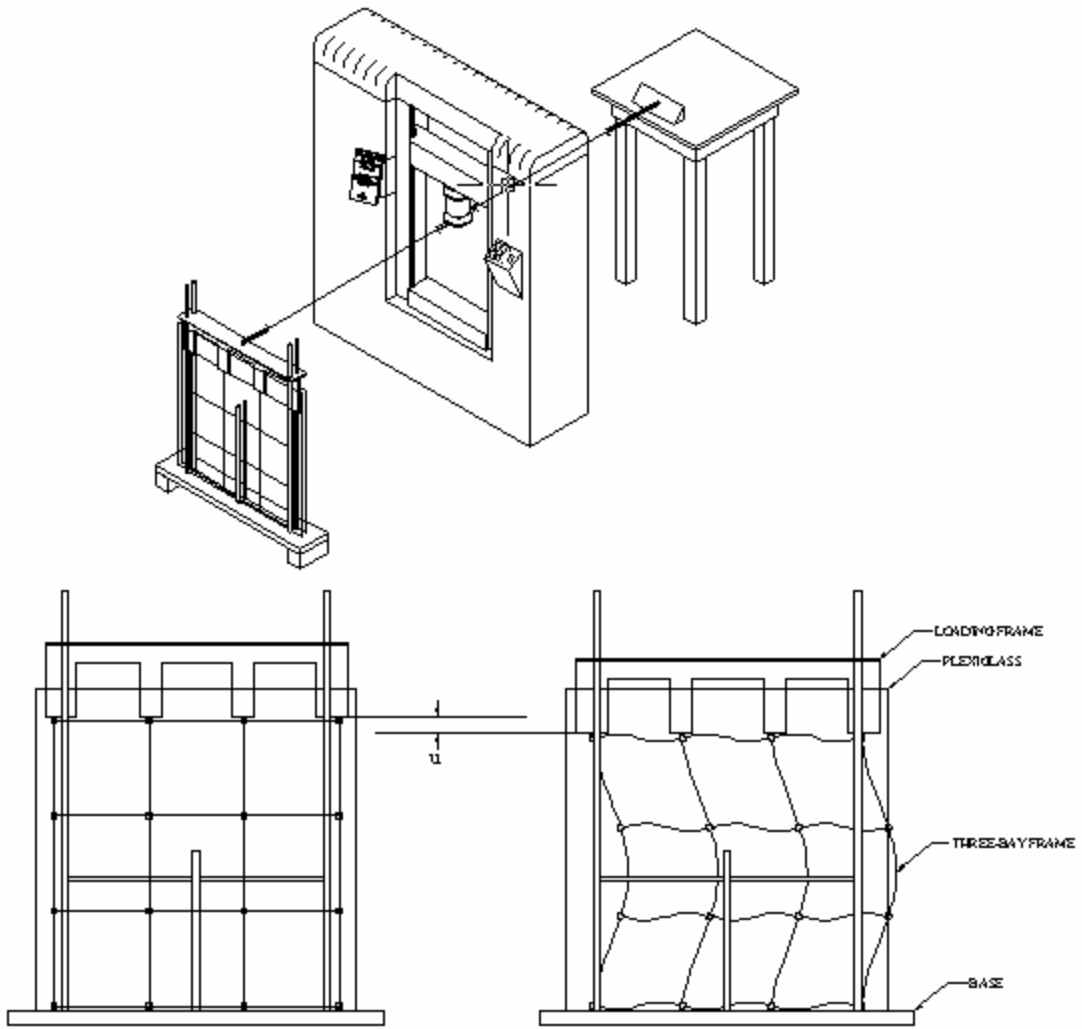
Figure 4. Experimental setup for the three-bay frame
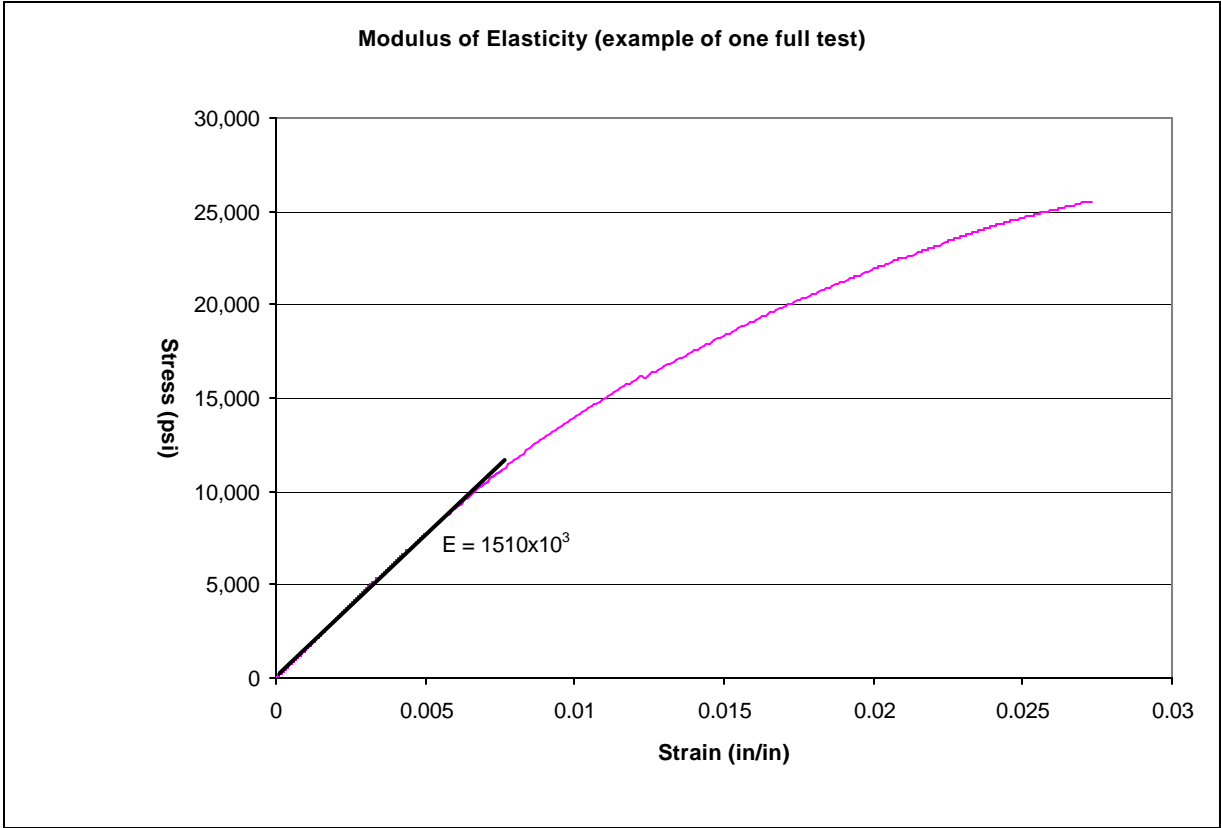
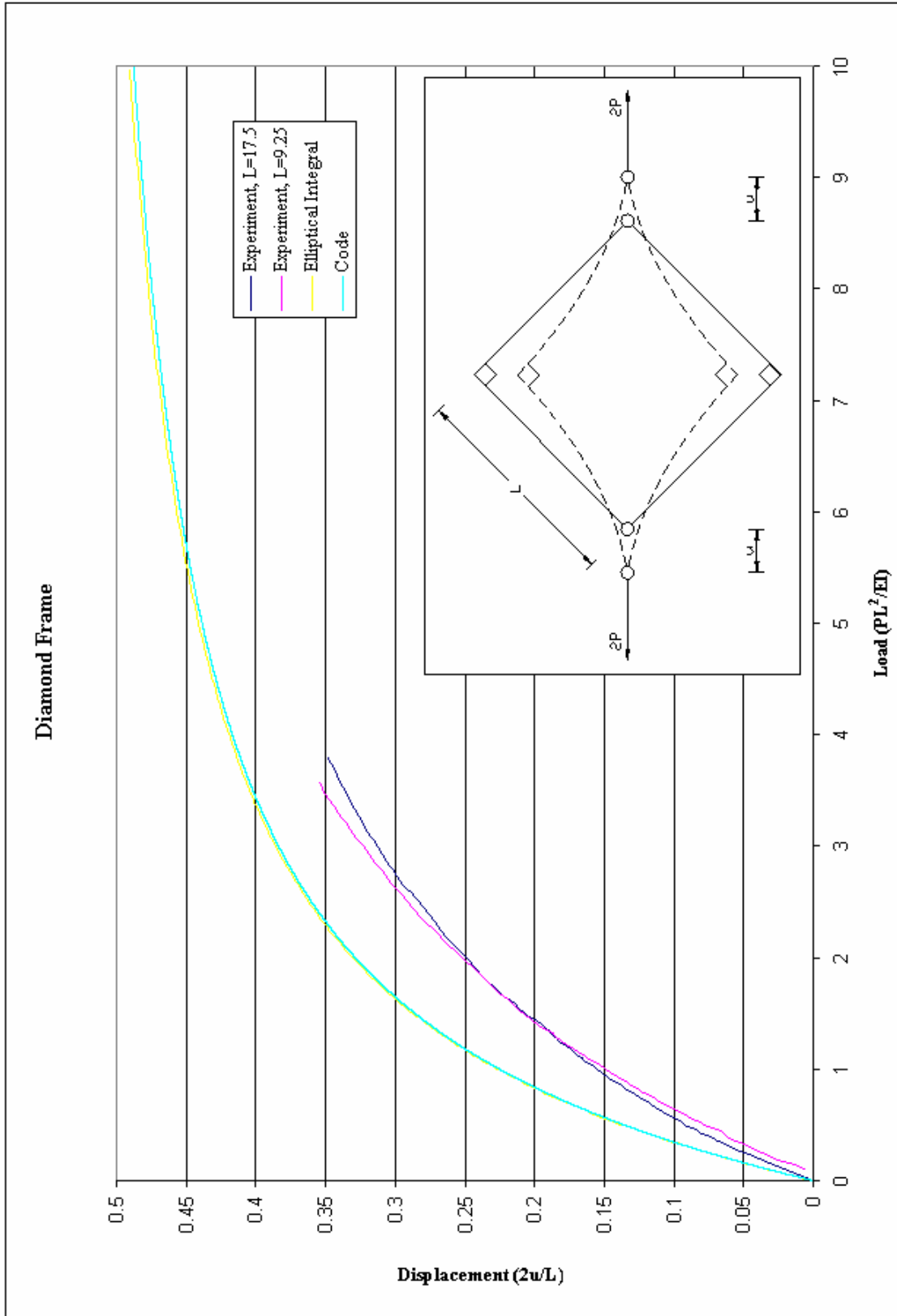**Figure 5.** Example of Stress-Strain curve of a wooden dowel
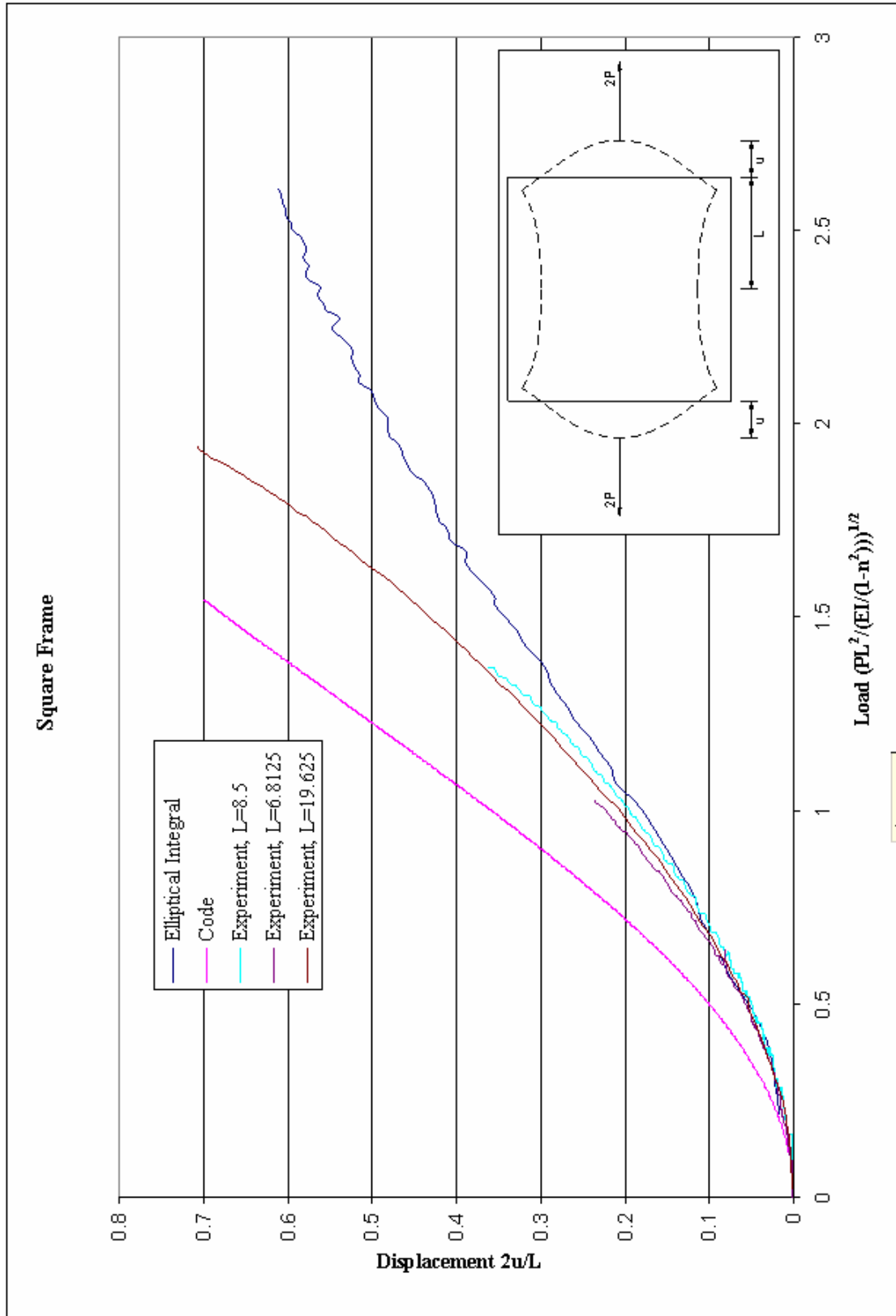
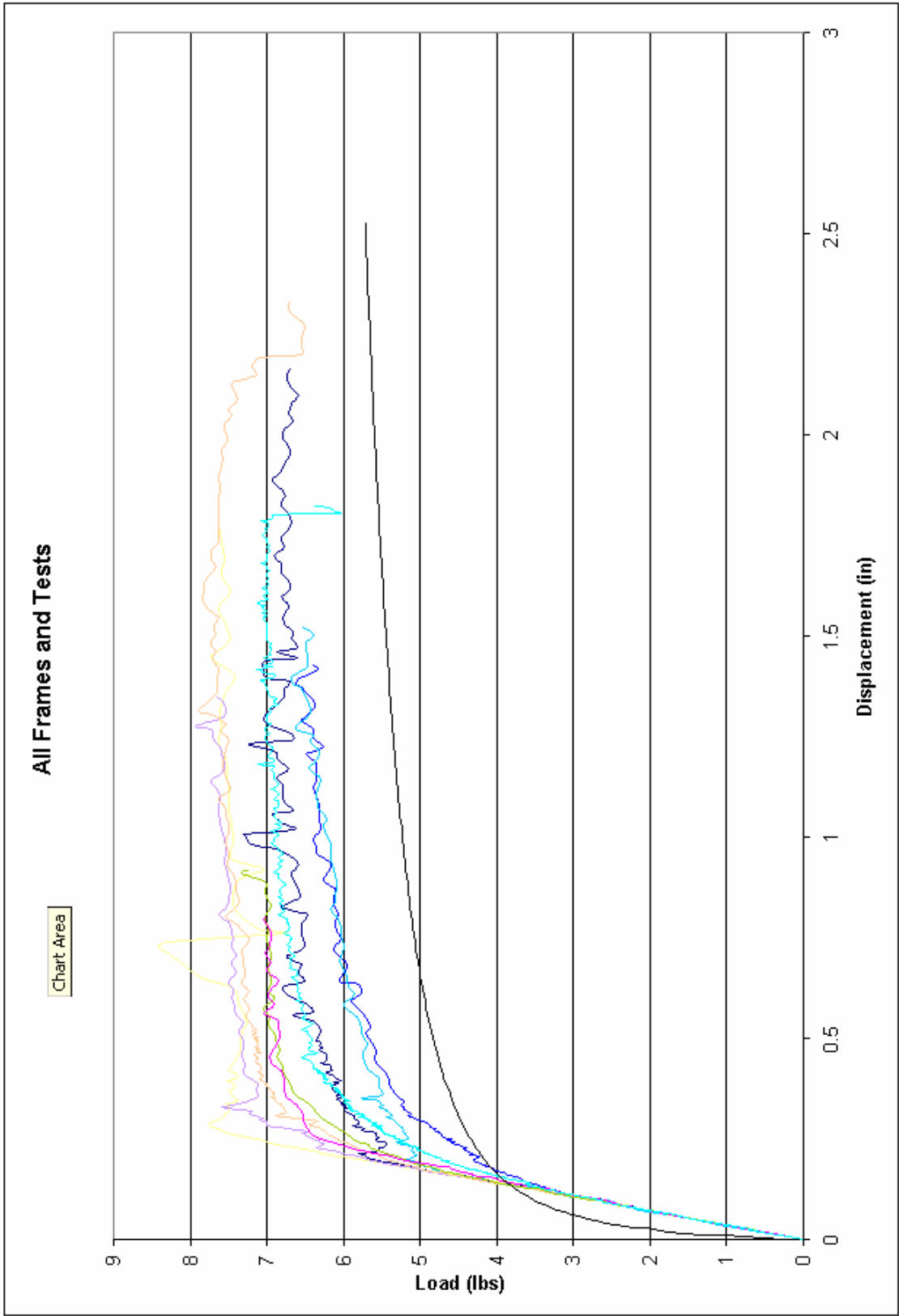**Figure 6.** Results of the diamond frame

Figure 7. Results of the square frame

Figure 8. Results of the three-bay frame